

Thermodynamic properties of rotating trapped ideal Bose gases

Yushan Li^{1,2} and Qiang Gu¹

¹ Department of Physics, University of Science and Technology Beijing, Beijing 100083, China

² Department of Physics, Heze University, Heze 274015, China

Ultracold atomic gases can be spined up either by confining them in rotating frame, or by introducing “synthetic” magnetic field. In this paper, thermodynamics of rotating ideal Bose gases are investigated within truncated-summation approach which keeps to take into account the discrete nature of energy levels, rather than to approximate the summation over single-particle energy levels by an integral as does in semi-classical approximation. Our results show that Bose gases in rotating frame exhibit much stronger dependence on rotation frequency than those in “synthetic” magnetic field. Consequently, BEC can be more easily suppressed in rotating frame than in “synthetic” magnetic field.

PACS numbers: 03.75.Hh, 05.30.Jp, 75.20.-g

I. INTRODUCTION

In the past few years, rotating Bose gases have been intensively studied in the context of trapped ultracold atomic gases [1, 2]. One may expect that rotation suppresses Bose-Einstein condensation (BEC). Like superconductors in magnetic field, vortices may be formed inside the condensate when it is rotated and the Abrikosov vortex lattice can even be observed [3–5]. More strikingly, rotating condensates in the fast-rotation limit are expected to exhibit novel quantum phases analogous to the quantum Hall state of electrons, if interactions between atoms are taken into account [6–10].

Earlier experiments to spin up neutral atomic gases are to confine them in a rotating frame [11–13]. More recently, the so-called “synthetic” magnetic field approach is developed [14–16], which creates an effective gauge potential \mathbf{A} for neutral atoms by means of optical field [17–19], instead of rotating the frame. In this case, atoms behave like charged particles in magnetic field. The “synthetic” magnetic field has already been realized in experiments and can be produced significantly large, which makes it hopefully to achieve the fast-rotating limit [14–16].

Although most research work on rotating Bose gases, both experimental and theoretical, focuses on the ground state properties or behaviors of rotating condensates, thermodynamic properties have also stimulated a number of interests [20–25]. The emphasis is mainly laid on Bose gases in the rotating frame. It is reported that the critical temperature decreases with the rotation frequency apparently [20, 21, 23]. Recent attention was also paid into the gases in “synthetic” magnetic field [23, 25].

The theoretical treatment in above works is mainly based on the semi-classical approximation (SCA), in which the energy spectrum is treated as a continuum and thus the summation over the discrete single-particle energy levels is converted into phase-space integrals. The SCA approach offers qualitatively accurate descriptions of thermodynamics of Bose gases without rotation through an extremely simple and efficient way [26].

Moreover, it is an effective approach to deal with Bose gases in the rotating frame [20, 21, 23, 24]. However, problem arises when the SCA approach is applied to ideal Bose gases in “synthetic” magnetic field [23]. For example, the BEC temperature in this case has no relation with the magnetic field. In the meanwhile, the Landau diamagnetism also keeps unchanging at all temperatures [23]. These unphysical results urge us to seek a more efficient treatment beyond the SCA approach.

The direct way to go beyond the SCA is to reconsider the discrete nature of the single-particle energy levels. Therefore, we compute the thermodynamic quantities of rotating trapped ideal Bose gases by performing the summation over discrete energy levels numerically by truncating the summation at certain order. This truncated-summation approach (TSA) produces reliable results and overcomes the disadvantage of the SCA when applying to ideal Bose gases in “synthetic” magnetic field.

This paper is organized as follows. Section 2 outlines main results on the basis of the semi-classical approximation and discusses briefly the problem that causes. We present numerical results based on the truncated-summation approach in Section 3 and then conclude in the last Section.

II. THE SEMI-CLASSICAL APPROXIMATION RESULTS

A. Trapped ideal Bose gases in the rotating frame

The single-particle Hamiltonian describing rotating neutral bosons with mass M trapped in harmonic potential can be written as

$$\begin{aligned}\hat{H} &= \frac{\mathbf{p}^2}{2M} + \frac{1}{2}M\omega_0^2(x^2 + y^2) + \frac{1}{2}M\omega_z^2z^2 - \Omega\hat{L}_z \\ &= \frac{(\mathbf{p} - \mathbf{A})^2}{2M} + \frac{1}{2}M(\omega_0^2 - \Omega^2)(x^2 + y^2) + \frac{1}{2}M\omega_z^2z^2,\end{aligned}\quad (1)$$

where \mathbf{p} is the momentum operator, \hat{L}_z is the operator of the orbital angular momentum, ω_0 and ω_z denote the transverse and axial frequencies of harmonic potential, Ω is the rotation frequency around the z axis. The vector potential in the symmetric gauge is $\mathbf{A} = (\mathbf{B} \times \mathbf{r})/2 = M(\Omega \times \mathbf{r})$, and $\mathbf{B} = 2M\Omega\bar{e}_z$ is the effective “magnetic” field.

The eigen-energy ε_{nlm} is given by

$$\varepsilon_{nlm} = (n + \frac{1}{2})\hbar\omega_z + (2l + |m| + 1)\hbar\omega_0 - m\hbar\Omega. \quad (2)$$

For simplicity, we can adopt a dimensionless treatment to eigen-values ε_{nlm} in units of $\hbar\omega_z$. One has

$$\bar{\varepsilon}_{nlm} = n + \frac{1}{2} + (2l + |m| + 1)\sigma - m\sigma\xi, \quad (3)$$

where $\bar{\varepsilon}_{nlm} = \varepsilon_{nlm}/(\hbar\omega_z)$, with the quantum numbers $n = 0, 1, 2, \dots$, $l = 0, 1, 2, \dots$, and $m = 0, \pm 1, \pm 2, \dots$. $\sigma = \omega_0/\omega_z$ and $\xi = \Omega/\omega_0$ denote the aspect ratio of harmonic trap and the dimensionless rotation frequency, respectively. The ground state energy of one particle is given by $\bar{\varepsilon}_0 = \bar{\varepsilon}_{000} = 1/2 + \sigma$.

The dimensionless thermodynamic potential is expressed as $\bar{\Omega} = \bar{\Omega}_T + \bar{\Omega}_0$. Thermodynamic potential for thermal particles $\bar{\Omega}_T$ reads

$$\begin{aligned} \bar{\Omega}_T &= \bar{T} \sum_{nlm} \ln \left[1 - \exp \left(\frac{\bar{\mu} - \bar{\varepsilon}_{nlm}}{\bar{T}} \right) \right] \\ &\simeq \bar{T} \int_0^\infty dn \int_0^\infty dl \int_{-\infty}^\infty dm \ln \left[1 - \exp \left(\frac{\bar{\mu} - \bar{\varepsilon}_{nlm}}{\bar{T}} \right) \right] \\ &= -\frac{\bar{T}^4}{\sigma^2(1-\xi^2)} g_4 \left(\frac{\bar{\varepsilon}_0 - \bar{\mu}}{\bar{T}} \right), \end{aligned} \quad (4)$$

where the summation over energy levels is replaced by direct integrals over all the quantum numbers. This is the so-called semi-classical approximation. Here $\bar{T} = k_B T/(\hbar\omega_z)$ is the dimensionless temperature, $\bar{\mu} = \mu/(\hbar\omega_z)$ is chemical potential, and $g_\gamma(z)$ is the polylogarithm function which obeys the relation $\partial g_\gamma(z)/\partial z = -g_{\gamma-1}(z)\partial z/\partial x$. For condensed bosons, $\bar{\Omega}_0$ is described by

$$\bar{\Omega}_0 = \frac{1}{\hbar\omega_z} \int d^3r \left\{ \frac{|\mathbf{D}\bar{\psi}|^2}{2M} + V(r)|\bar{\psi}|^2 - \mu|\bar{\psi}|^2 \right\}, \quad (5)$$

with $\mathbf{D}\bar{\psi} = \hbar\nabla\bar{\psi} + i\mathbf{A}\bar{\psi}$. $\bar{\psi}$ is a background field and $V(r)$ represents trapping potential.

All thermodynamic quantities can be obtained from the thermodynamic potentials. The BEC temperature is given by

$$\bar{T}_C = \left(\frac{\omega_0^2 - \Omega^2}{\omega_z^2 g_3(0)} N \right)^{\frac{1}{3}} = \left[\frac{\sigma^2(1-\xi^2)}{g_3(0)} N \right]^{\frac{1}{3}}. \quad (6)$$

Note that BEC temperature of Bose gases in the rotating frame decreases with rotation frequency increasing.

When the rotation frequency Ω approaches to the trap frequency ω_0 (called the fast-rotating limit), the BEC does no longer take place [20, 21, 23].

The condensate fraction is written as

$$\frac{N_0}{N} = 1 - \left(\frac{\bar{T}}{\bar{T}_C} \right)^3. \quad (7)$$

This is formally identical with the expression of non-rotating harmonically trapped Bose gases in three dimensional space. The impact of rotating effect on the condensate fraction mainly comes from Eq. (6).

If looking upon it as some effective magnetic field, ξ may induce “magnetization”, which reads

$$\bar{M} = -\frac{\partial \bar{\Omega}}{\partial \xi} = -N\xi. \quad (8)$$

The value of magnetization is negative, reflecting that Bose gases in the rotating frame exhibit the Landau diamagnetism. We point out that the magnetization keeps invariant at all temperatures [23], conflicting with our established intuition which the magnetization varies with the temperature and diamagnetism is stronger at lower temperatures.

B. Trapped ideal Bose gases in “synthetic” magnetic field

The effective Hamiltonian for a trapped atom in “synthetic” magnetic field can be expressed as follows,

$$\hat{H} = \frac{(\mathbf{p} - \mathbf{A})^2}{2M} + \frac{1}{2}M\omega_0^2(x^2 + y^2) + \frac{1}{2}M\omega_z^2 z^2, \quad (9)$$

which looks like that of charged particles in the magnetic field with \mathbf{A} representing “synthetic” gauge potential. And the energy levels are given by

$$\bar{\varepsilon}_{nlm} = n + \frac{1}{2} + (2l + |m| + 1)\sqrt{\sigma^2 + \bar{B}^2} - m\bar{B}, \quad (10)$$

where $\sigma = \omega_0/\omega_z$, $\bar{B} = \omega_L/\omega_z$, and ω_L denotes the Larmor frequency.

We can directly present the analytical expression of BEC temperature within SCA framework according to Ref. [23],

$$\bar{T}_C = \left(\frac{\sigma^2 N}{g_3(0)} \right)^{\frac{1}{3}}. \quad (11)$$

Obviously, BEC temperature is irrelevant to “synthetic” magnetic field, only determined by the frequency of harmonic potential and the particle number.

Diamagnetization in “synthetic” magnetic field \bar{B} can be calculated similarly to the rotating frame case,

$$\bar{M} = -\frac{\partial \bar{\Omega}}{\partial \bar{B}} = -\frac{N\bar{B}}{\sqrt{\sigma^2 + \bar{B}^2}}. \quad (12)$$

It vanishes as $\bar{B} \rightarrow 0$, but seems to have no relation with the temperatures. Therefore, a correction to thermodynamics of the SCA is needed.

C. Problem with the semi-classical approximation

As already studied [20, 21, 23, 24], the SCA is very useful in calculation the thermodynamics of Bose gases without rotation and those in the rotating frame. It also provides a good description of thermodynamic quantities such as the BEC temperature, condensate fraction, and specific heat. Nevertheless, the magnetization expressed in Eq. (8) indicates that it fails in exploring magnetic properties. The problem goes more serious in the case of Bose gases in “synthetic” magnetic field. Neither the BEC temperature nor the diamagnetization is correctly calculated, as suggested in Eqs. (11) and (12).

The failure of SCA in dealing with magnetic properties of quantum gases reminds us to recall the Bohr-van Leeuwen theorem. Within this semi-classical approximation, the grand-canonical free energy of the ideal Bose gas reads [21]

$$\begin{aligned}\mathcal{F} &= N_0(\mu_c - \mu) - \sum_{j=1}^{\infty} \frac{1}{j\beta} \exp\{-\beta[H_j(\mathbf{x}, \mathbf{P}) - \mu]\} \\ &= N_0(\mu_c - \mu) - \frac{1}{\beta} \int \frac{d^3x d^3P}{(2\pi\hbar)^3} \exp\{-\beta[H(\mathbf{x}, \mathbf{P}) - \mu]\},\end{aligned}\quad (13)$$

where μ_c denotes the critical chemical potential at which the condensation emerges. The energy levels H_j are replaced by the classical Hamiltonian

$$\hat{H} = \frac{\mathbf{P}^2}{2M} + V(\mathbf{x}, \Omega). \quad (14)$$

where $\mathbf{P} = \mathbf{p} - \mathbf{A}$. Therefore, the gauge potential \mathbf{A} in the first term of Hamiltonians (1) and (9) disappears in the integral. In Hamiltonian (1), the rotation is still partially embodied in the second term by the rotation frequency Ω , while in Hamiltonian (9) the rotation information is completely drowned.

To retrieve the lost information regarding the rotation, the discrete feature of energy levels must be held back. In the following section, we will calculate summations over energy levels directly, rather than converting the summation into integrals.

Recently, EI-Badry has calculated the field dependence of BEC temperature and the temperature dependence for synthetic magnetization base on a modified semi-classical approximation. He obtains the decrease of \bar{T}_C with increasing the field and \bar{M} with the temperature [25]. Their results include simultaneously corrections to quantities arising from the finite size and interatomic interaction effects. Quantization feature of energy levels is still not taken into account.

III. NUMERICAL RESULTS: THE TRUNCATED-SUMMATION APPROACH

We first describe the method employed in this section. Generally, thermodynamic quantities derived from ther-

modynamic potential is an infinite summation over all the energy levels. Take the number of particles for example, $N = -\partial\bar{\Omega}/\partial\bar{\mu}$, which yields

$$N_T = \sum_{nlm} \{\exp[(\bar{\epsilon}_{nlm} - \bar{\mu})/\bar{T} - 1]\}^{-1} \quad (15)$$

and

$$N_0 = -\frac{\partial\bar{\Omega}_0}{\partial\bar{\mu}} = |\bar{\psi}|^2, \quad (16)$$

corresponding to the number of thermal and condensed bosons, respectively. Here $\bar{\epsilon}_{nlm}$ denotes energy levels expressed in Eq. (3) for the rotating frame case and Eq. (10) for “synthetic” field case, respectively.

Unfortunately, it is impossible to derive an analytical expression of the infinite summation. Therefore we perform numerical calculations by truncating the summation at certain order of energy levels. That is to say, higher energy levels are neglected. Basically, this truncated-summation approach is reasonable because the quantum effect we concern occurs at low temperature and thus the higher energy levels are seldom occupied.

A. Trapped ideal Bose gases in the rotating frame

Admittedly, the more energy levels are considered, the more accurate the obtained results are, and the higher the computational cost is. In order to acquire satisfactory precision of the results, we need to choose an appropriate cut-off-level of the energy, at which the summation is truncated. There are three quantum numbers to describe the energy level, n , l and m . For simplicity, we set that the summation over each quantum number is cut off at the same maximum value n_{max} . That is, the scopes of quantum numbers n, l, m are defined as $n \in [0, n_{max}]$, $l \in [0, n_{max}]$, $m \in [-n_{max}, n_{max}]$.

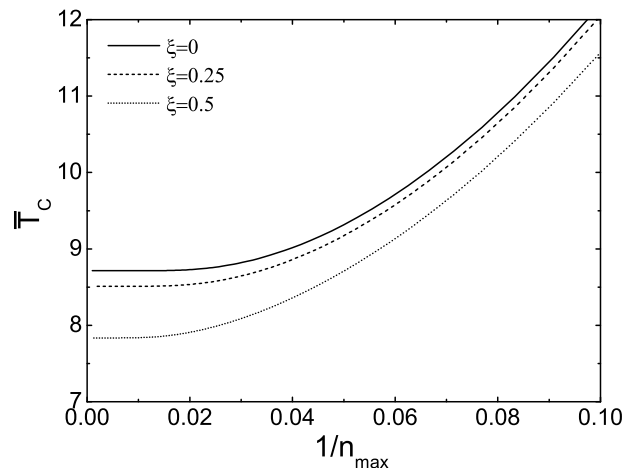


FIG. 1: Plots of the BEC temperature \bar{T}_C versus the inverse of the truncated order n_{max} for trapped Bose gases in the rotating frame.

Let's first calculate the BEC temperature \bar{T}_C according to Eq. (15). The particle number is set as $N = 1000$ and harmonic trap is set to be isotropic ($\sigma = 1$). As can be seen from Fig. 1, \bar{T}_C drops quickly as n_{max} increases when n_{max} is small, which means that the summation does not converge. When $n_{max} \geq 100$, \bar{T}_C remains stable with n_{max} increasing. The summation is already convergent because considering more higher energy levels does not lead to visible changes to the result. In following calculations, we choose $n_{max} = 1000$ in order to ensure the precision of results, in which case the total energy levels being considered are up to 10^9 .

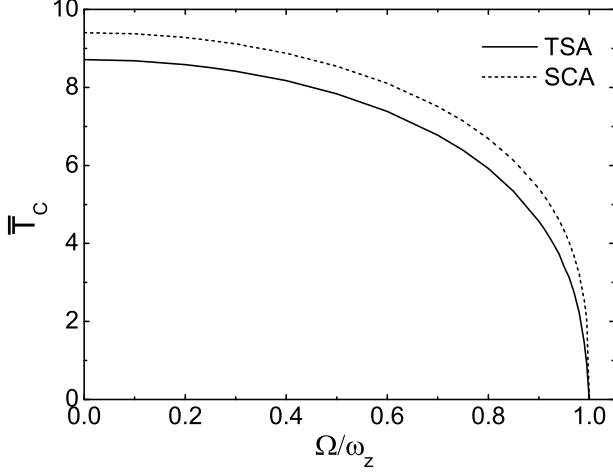


FIG. 2: The BEC temperature as a function of rotation frequency. The solid and short dashed lines denote the TSA and SCA results, respectively.

We calculated the BEC temperature as a function of the rotation frequency. The TSA and SCA results are compared in Fig. 2. The TSA result is lower than the SCA one, but the difference is negligible. Particularly, both results drop down to zero when $\Omega \rightarrow \omega_0$. At this point, the system reaches the fast-rotating limit and BEC is completely suppressed.

The condensate fraction for the $\xi = 0.5$ case versus the normalized temperature is plotted in Fig. 3. The temperature dependence of N_0/N deviates slightly from the $1 - (\bar{T}/\bar{T}_C)^3$ law predicted by the SCA. Interestingly, normalized-temperature dependence of N_0/N at different rotating frequencies obeys almost the same law, as demonstrated in the inset of Fig. 3.

Figure 4 shows the specific heat, \bar{C} , which is given in the summation form

$$\bar{C} = \sum_{nlm} \frac{\bar{\varepsilon}_{nlm}}{\bar{T}^2} \frac{\exp\left(\frac{\bar{\varepsilon}_{nlm} - \bar{\mu}}{\bar{T}}\right) \left[\bar{T} \frac{\partial \bar{\mu}}{\partial \bar{T}} + \bar{\varepsilon}_{nlm} - \bar{\mu}\right]}{\left[\exp\left(\frac{\bar{\varepsilon}_{nlm} - \bar{\mu}}{\bar{T}}\right) - 1\right]^2}. \quad (17)$$

For $\bar{T} \leq \bar{T}_C$, the chemical potential $\bar{\mu}$ is equal to the ground state energy $\bar{\varepsilon}_0$. \bar{C} exhibits discontinuity at the critical temperature. It tends to zero at the low temperature limit $\bar{T} \rightarrow 0$ and Dulong-Petit specific heat at high temperature region. TSA results are larger below \bar{T}_C , but smaller above \bar{T}_C than the SCA results.

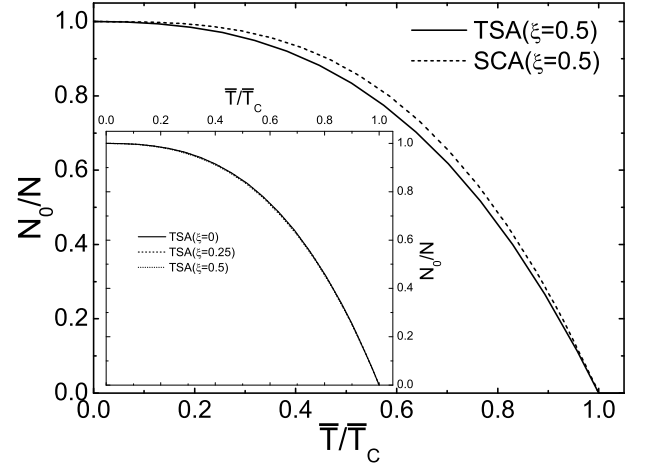


FIG. 3: Condensate fraction versus the normalized temperature at $\xi = 0.5$. Inset: TSA results for different rotation frequencies.

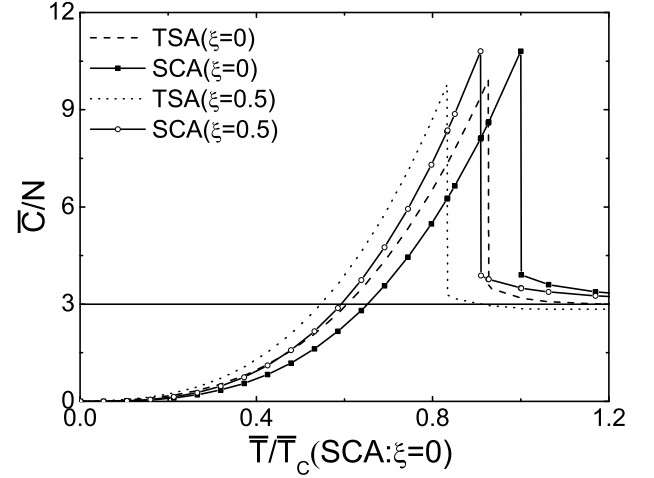


FIG. 4: The per-particle specific heat versus temperature which is in unit of the SCA BEC temperature at $\xi = 0$. The horizontal solid line indicates the Dulong-Petit law.

Above results suggest that the TSA only brings about small corrections to the SCA. We proceed to check the magnetization, which in the summation form is given by

$$\bar{M} = -N_0 \xi - \sum_{nlm} \frac{(2l + |m| + 1)\xi - m}{\exp\left[\frac{(\bar{\varepsilon}_{nlm} - \bar{\mu})}{\bar{T}}\right] - 1}. \quad (18)$$

The obtained result shown in Fig. 5 suggests the TSA correction to diamagnetization comes dramatically significant. Distinct from the SCA result which keeps a constant at all temperatures, \bar{M} becomes varying with \bar{T} , particularly at low temperature. The SCA result just amounts to the minimum value of the TSA result. \bar{M} drops quickly with \bar{T} dreading and achieves its maximum at $\bar{T} = 0$. This behavior means that the diamagnetism is stronger at lower temperatures especially below the transition temperature. Above the BEC temperature, the $\bar{M} - \bar{T}$ line becomes flatten out, and tends to zero at higher temperature. This suggests that the rotation

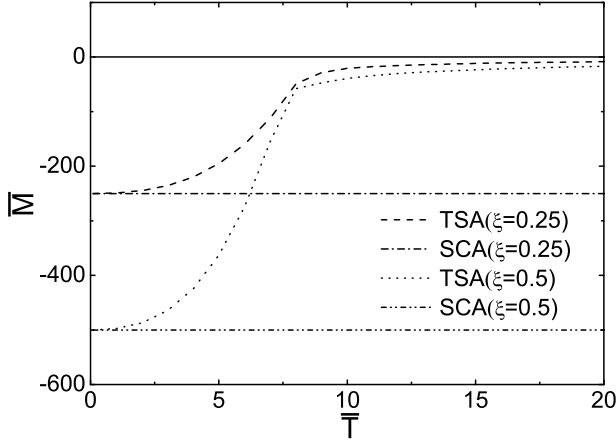


FIG. 5: Magnetization versus temperature. The solid line indicates the case of non-rotating states.

effect is sorely suppressed by thermal fluctuations.

B. Trapped ideal Bose gases in “synthetic” magnetic field

In comparison to the gas in the rotating frame, less attention has been paid to the Bose gas in “synthetic” magnetic field [23, 25]. Plausibly, the two systems might exhibit similar behaviors, since their Hamiltonians resemble each other. However, the results based on SCA have revealed that they show more differences than similarities. Moreover, according to the analysis in Sec. II C, the SCA is more unapplicable to the Bose gas in “synthetic” magnetic field. Thus it is in more need of treatment beyond SCA.

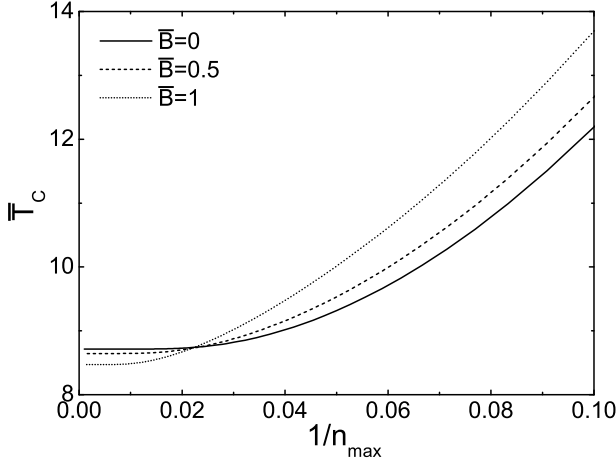


FIG. 6: The BEC temperature \bar{T}_C versus the inverse of the truncated order n_{max} at different “synthetic” magnetic field \bar{B} .

Once again, we need to verify the accuracy and reliability of the TSA. Figure 6 shows the $\bar{T}_C - 1/n_{max}$ curve at different given fields. It should be noted that convergency of the summation becomes worse in stronger

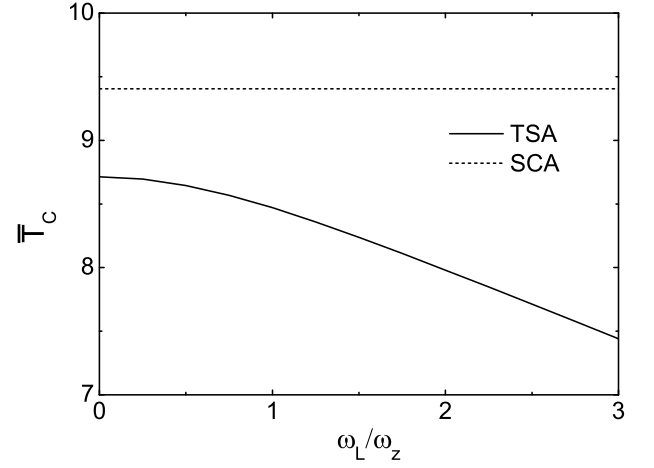


FIG. 7: The BEC temperatures as a function of ω_L/ω_z . The solid and short dashed lines show the TSA and SCA results, respectively.

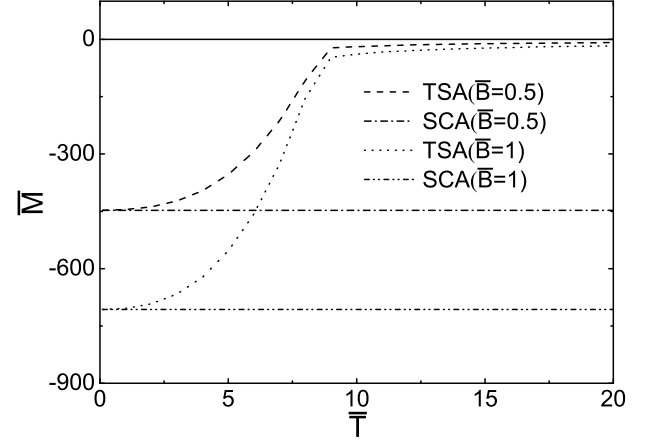


FIG. 8: Magnetization versus temperature for different “synthetic” magnetic field. The solid line denotes the zero-field case.

magnetic field, and thus we need a larger n_{max} . And again we judge that $n_{max} = 1000$ is sufficient to ensure acceptable accuracy.

Figure 7 plots the BEC temperature, \bar{T}_C , as a function of “synthetic” magnetic field, \bar{B} . The “synthetic” field-dependence of \bar{T}_C takes on completely different characteristics from that within the SCA, for which \bar{T}_C has no relation with \bar{B} . The present result appears more reasonable and keeps consistent in superconductivity when exposed to a magnetic field, where the transition temperature decreases as the magnetic field is strengthened. We wish to point out that BEC temperature of the trapped Bose gas either in the rotating frame or in “synthetic” magnetic field decreases with the rotation frequency ξ or “synthetic” magnetic field \bar{B} . Nevertheless, \bar{T}_C drops more quickly in the former case, as indicated in Figs. 2 and 7.

As shown in Fig. 7, $\bar{T}_C \approx 7.4$ at $\bar{B} = 3$, which is still quite large. Based on present results, we suspect that $\bar{T}_C \rightarrow 0$ at about $\bar{B} = 18$ according to the decreasing

trend of the BEC temperature with “synthetic” magnetic field. However, within the current truncated energy levels, we can not find $\bar{T}_C \rightarrow 0$. This might be owing to the fact that n_{max} is not large enough to produce convincing numerical results at that large field. If stronger field B is considered, we need to choose a larger n_{max} .

Figure 8 shows the “synthetic” diamagnetism calculated from the following formula,

$$\bar{M} = -\frac{N_0 \bar{B}}{\sqrt{\sigma^2 + \bar{B}^2}} - \sum_{nlm} \frac{(2l + |m| + 1) \frac{\bar{B}}{\sqrt{\sigma^2 + \bar{B}^2}} - m}{\exp[(\bar{\epsilon}_{nlm} - \bar{\mu})/\bar{T}] - 1}. \quad (19)$$

Its feature is similar to that of the trapped Bose gas in the rotating frame. It is by no means a constant with temperature as the SCA predicted. The “synthetic” magnetization \bar{M} decreases as the temperature is lowered, reaching its maximum value at $\bar{T} = 0$. Magnetization \bar{M} is stronger and negative at larger “synthetic” magnetic field \bar{B} below the BEC temperature. Our results provide a theoretical support for the current experiment [27].

C. Comparison with other improvements to the semi-classical approximation

It is worth noting that two other relevant approaches have already been proposed to improve the SCA by taking into account, more or less explicitly, the quantization feature of energy levels [22, 28]. In Ref. [22], Balaž *et al.* developed an efficient ultra-fast converging path-integral approach on the basis of precise single-particle energy spectrum and obtained more reasonable results than semi-classical calculations, in particular for smaller particle numbers. The other approach retrieves the lost information in SCA by considering higher order corrections when replacing summations by an integral [28]. Thermodynamic properties of harmonically trapped ideal Bose gases without rotation were calculated analytically.

Relatively, the TSA is a quite simple but already effective approach to go beyond the SCA. In order to demonstrate this point, we give a direct comparison between the TSA result and the first (the first two) finite-size corrections in Ref. [28], as shown in Fig. 9. It is clearly shown that the TSA correction yields very good agreement with the first two finite-size correction even for small particle numbers.

IV. CONCLUSIONS

In this paper, we study thermodynamic properties of the rotating trapped ideal Bose gas numerically using a truncated-summation approach. This approach conserves the discrete feature of energy levels in contrast

to the semi-classical approximation, thus it helps to account for quantum effects of the system, e.g., the effect

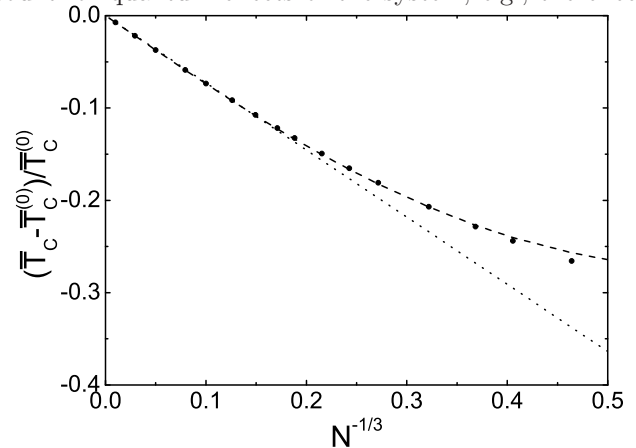


FIG. 9: Finite-size corrections $(\bar{T}_C - \bar{T}_C^{(0)})/\bar{T}_C^{(0)}$ versus $N^{-1/3}$. The bullets denote the TSA correction. \bar{T}_C and $\bar{T}_C^{(0)}$ denote the BEC temperature for ideal gases without rotation within the TSA and SCA, respectively. The dotted (dashed) line corresponds to the first (the first two) finite-size corrections which is taken from Eq. (32) in Ref. [28].

tive “magnetization” resulted from the rotation. The obtained results indicate that the “diamagnetization” turns significantly stronger below the BEC temperature than above, coinciding with our intuition established in superconductivity.

We perform calculations of the BEC temperature as a function of the rotation frequency for bosons spined up both by the rotating frame and “synthetic” magnetic field. In both cases, the BEC temperature decreases with the increasing rotation frequency or “synthetic” magnetic field, which suggests that the rotation tends to destroy BEC. The decrease seems much slower in the latter case. It probably implies that more stronger “synthetic” magnetic field is needed in order to drive the system to the fast-rotating limit. Moreover, the specific heat is briefly discussed. Similar to the SCA result, the specific heat shows discontinuity at the BEC temperature and tends to a constant in high temperature region.

Acknowledgements

This work is supported by the National Key Basic Research Program of China (Grant No. 2013CB922000), the National Natural Science Foundation of China (Grant No. 11074021) and the Fundamental Research Funds for the Central Universities of China. QG acknowledges support from the China Scholarship Council and the hospitality of the Rudolf Peierls Centre for Theoretical Physics, University of Oxford.

-
- [1] I. Bloch, J. Dalibard, W. Zwerger, *Rev. Mod. Phys.* **80** (2008) 885.
 - [2] A. L. Fetter, *Rev. Mod. Phys.* **81** (2009), 647 and references therein.
 - [3] J. R. Abo-Shaeer, C. Raman, J. M. Vogels, W. Ketterle, *Science* **292** (2001) 476.
 - [4] V. Bretin, S. Stock, Y. Seurin, J. Dalibard, *Phys. Rev. Lett.* **92** (2004) 050403.
 - [5] V. Schweikhard, I. Coddington, P. Engels, V. P. Mogen-dorff, E. A. Cornell, *Phys. Rev. Lett.* **92** (2004) 040404.
 - [6] T.-L. Ho, *Phys. Rev. Lett.* **87** (2001) 060403.
 - [7] U. R. Fischer, G. Baym, *Phys. Rev. Lett.* **90** (2003) 140402.
 - [8] G. Watanabe, G. Baym, C. J. Pethick, *Phys. Rev. Lett.* **93** (2004) 190401.
 - [9] N. K. Wilkin, J. M. F. Gunn, *Phys. Rev. Lett.* **84** (2000) 6.
 - [10] N. R. Cooper, N. K. Wilkin, J. M. F. Gunn, *Phys. Rev. Lett.* **87** (2001) 120405.
 - [11] K. W. Madison, F. Chevy, W. Wohlleben, J. Dalibard, *Phys. Rev. Lett.* **84** (2000) 806.
 - [12] P. C. Haljan, I. Coddington, P. Engels, E. A. Cornell, *Phys. Rev. Lett.* **87** (2001) 210403.
 - [13] E. Hodby, G. Hechenblaikner, S. A. Hopkins, O. M. Maragò, C. J. Foot, *Phys. Rev. Lett.* **88** (2002) 010405.
 - [14] Y.-J. Lin, R. L. Compton, A. R. Perry, W. D. Phillips, J. V. Porto, I. B. Spielman, *Phys. Rev. Lett.* **102** (2009) 130401.
 - [15] Y.-J. Lin, R. L. Compton, K. Jiménez-García, J. V. Porto, I. B. Spielman, *Nature* **462** (2009) 628.
 - [16] Y.-J. Lin, R. L. Compton, K. Jiménez-García, W. D. Phillips, J. V. Porto, I. B. Spielman, *Nat. Phys.* **7** (2011) 531.
 - [17] J. Higbie, D. M. Stamper-Kurn, *Phys. Rev. Lett.* **88** (2002) 090401.
 - [18] D. Jaksch, P. Zoller, *New J. Phys.* **5** (2003) 56; A. S. Sørensen, E. Demler, M. D. Lukin, *Phys. Rev. Lett.* **94** (2005) 086803.
 - [19] G. Juzeliūnas, P. Öhberg, *Phys. Rev. Lett.* **93** (2004) 033602; G. Juzeliūnas, J. Ruseckas, P. Öhberg, M. Fleischhauer, *Phys. Rev. A* **73** (2006) 025602.
 - [20] S. Stringari, *Phys. Rev. Lett.* **82** (1999) 4371.
 - [21] S. Kling, A. Pelster, *Phys. Rev. A* **76** (2007) 023609.
 - [22] A. Balaž, I. Vidanović, A. Bogojević, A. Pelster, *Phys. Lett. A* **374** (2010) 1539.
 - [23] J. H. Fan, Q. Gu, W. Guo, *Chin. Phys. Lett.* **28** (2011) 060306.
 - [24] A. S. Hassan, A. M. El-Badry, S. S. M. Soliman, *Eur. Phys. J. D* **64** (2011) 465.
 - [25] A. M. El-Badry, *Turk. J. Phys.* **37** (2013) 30.
 - [26] V. Bagnato, D. E. Pritchard, D. Kleppner, *Phys. Rev. A* **35** (1987) 4354.
 - [27] B. Pasquiou, E. Maréchal, L. Vernac, O. Gorceix, B. Laburthe-Tolre, *Phys. Rev. Lett.* **108** (2012) 045307.
 - [28] B. Klünder, A. Pelster, *Eur. Phys. J. B* **68** (2009) 457.